

RESEARCH PAPER



# Downregulation of cancer-associated fibroblast exosome-derived miR-29b-1-5p restrains vasculogenic mimicry and apoptosis while accelerating migration and invasion of gastric cancer cells via immunoglobulin domain-containing 1/zonula occluden-1 axis

Chenqu Wu\*, Deming Li\*, Xun Cheng, Hao Gu, Yanqing Qian, and Li Feng

Endoscopy Center, Minhang Hospital, Fudan University, Shanghai, China

## ABSTRACT

**Background:** Cancer-associated fibroblast (CAF) exosomal miRNAs have gradually a hot spot in cancer therapy. This study mainly explores the effect of CAF-derived exosomal miR-29b-1-5p on gastric cancer (GC) cells.

**Methods:** CAFs and exosomes were identified by Western blot and transmission electron microscopy. CAF-derived exosomes-GC cells co-culture systems were constructed. Effects of CAF-derived exosomal miR-29b-1-5p on GC cells were determined by cell counting kit-8, flow cytometry, wound healing, Transwell assays and Western blot. The relationship between miR-29b-1-5p and immunoglobulin domain-containing 1 (VSIG1) was assessed by TargetScan, dual-luciferase reporter and RNA immunoprecipitation (RIP) experiments. The interaction between VSIG1 and zonula occluden-1 (ZO-1) was detected by co-immunoprecipitation. Expressions of miR-29b-1-5p, VSIG1 and ZO-1 were determined by quantitative real-time PCR. Vascular mimicry (VM) was detected using immunohistochemistry and tube formation assays. Rescue experiments and xenograft tumor assays were used to further determine the effect of CAF-derived exosomal miR-29b-1-5p/VSIG1 on GC.

**Results:** VM structure, upregulation of miR-29b-1-5p, and downregulation of VSIG1 and ZO-1 were shown in GC tissues. MiR-29b-1-5p targeted VSIG1, which interacted with ZO-1. CAF-derived exosomal miR-29b-1-5p inhibitor suppressed the viability, migration, invasion and VM formation, but promoted the apoptosis of GC cells. MiR-29b-1-5p inhibitor increased levels of VSIG1, ZO-1 and E-cadherin, whilst decreasing levels of VE-cadherin, N-cadherin and Vimentin in vitro and in vivo, which however was partially reversed by shVSIG1. Downregulation of CAF-derived exosomal miR-29b-1-5p impeded GC tumorigenesis and VM structure in vivo by upregulating VSIG1/ZO-1 expression.

**Conclusion:** Downregulation of CAF-derived exosomal miR-29b-1-5p inhibits GC progression via VSIG1/ZO-1 axis.

## ARTICLE HISTORY

Received 24 June 2022  
Revised 1 November 2022  
Accepted 2 May 2023

## KEYWORDS

Cancer-associated fibroblast; gastric cancer; MiR-29b-1-5p; exosome, VSIG1

## Introduction


Gastric cancer (GC) is a highly prevalent malignant tumor in the digestive system and the third lethal cancer [1]. Despite the current progress in the treatment of GC, the survival rate is still limited [2]. Therefore, in-depth understanding on the pathological mechanism of GC development is of great value for the search on GC diagnostic markers and therapeutic targets. In addition to the conventional biological properties of tumor cells such as malignant proliferation, migration and invasion, the blood supply also accelerates cancer progression and metastasis [3,4].

Vasculogenic mimicry (VM), a vascular-like network formed by highly aggressive tumor cells, plays a pivotal role in promoting cancer progression in GC [5,6]. Therefore, investigating VM formation and other biological functions in GC may further clarify the role of target genes.

In the past decade, the concept of tumor microenvironment has gradually attracted the attention of researchers [7,8]. Cancer-associated fibroblasts (CAFs), a type of important interstitial cells in the tumor microenvironment, play critical roles in tumor metastasis, angiogenesis

**CONTACT** Yanqing Qian ✉ [qianyanqing@fudan.edu.cn](mailto:qianyanqing@fudan.edu.cn); Li Feng ✉ [feng\\_li@fudan.edu.cn](mailto:feng_li@fudan.edu.cn) Endoscopy Center, Minhang Hospital, Fudan University, 170 Xin-Song Road, Shanghai 201199, China

\*These authors contributed equally to this work.

 Supplemental data for this article can be accessed online at <https://doi.org/10.1080/15384101.2023.2231740>.

and other processes through paracrine processes [8–10]. As a “communication factor”, exosomes can regulate target cells by transporting active substances such as microRNAs (miRNAs/miRs) in their source cells [11]. Continuing studies have demonstrated that exosomes are closely related to GC development, including metastasis, angiogenesis, immune escape, and drug resistance [11,12]. Deng et al. revealed that GC cell-derived exosomes have the abilities to induce mesothelial cell apoptosis and mesothelial-mesenchymal transition, and also promote the metastasis of GC cells in the peritoneal cavity [13]. Furthermore, exosome-derived miRNA has good stability and may become a new tumor marker [14]. Liu et al. found that gastric cancer cells can transfer miR-451 to T cells through exosomes, inhibit the expression of adenosine 5'-monophosphate (AMP)-activated protein kinase (AMPK), enhance the activity of mammalian target of rapamycin (mTOR), and induce Th17 differentiation [15]. Yang et al. reported that exosomal miR-423-5p in GC cells promotes GC growth and metastasis by inhibiting suppressor of fused protein (SUFU) expression [16]. Therefore, studying exosome-derived miRNAs is expected to open up new therapeutic space for GC patients.

Based on previous research, we analyzed the GSE126399 dataset and obtained some abnormally expressed miRNAs in liver cirrhosis-related benign ascites and GC-related malignant ascites. Among the top ten miRNAs, miR-29b-1-5p is found to be highly expressed in GC (exosomes) [17], but the specific mechanism still needs to be further explored. The abnormally high expression of miR-29b-1-5p perhaps serves as one of the driving factors for the occurrence and development of GC. MiR-29b-1-5p also exhibits oncogenic activity in oral squamous cell carcinoma [18], which adds confidence to our upcoming studies. In addition, to gain insight into the mechanism of miR-29b-1-5p, the genes with targeted binding sequences were analyzed by means of bioinformatics. Among them, immunoglobulin domain-containing 1 (VSIG1) is predicted to be targeted by miR-29b-1-5p and is lowly expressed in GC [19]. Therefore, this study mainly adopts the miR-29b-1-5p/VSIG1 axis as the starting point to unveil the effect of

CAF-derived exosomal miR-29b-1-5p on the biological function of GC cells.

## Materials and methods

### Ethics statement

GC tissue, para-cancerous tissues (adjacent normal tissues) and blood samples were collected from 57 gastric cancer patients in Central Hospital of Minhang District in Shanghai, with 18 non-metastatic GC patients and 39 metastatic GC patients. The metastatic tissues were harvested from primary tumors of GC patients with metastatic disease. Venous blood samples from 13 healthy volunteers were also obtained. All clinical experiments and animal assays were approved by Medical Ethics Committee of Central Hospital of Minhang District in Shanghai [Medical Ethics Committee (2021) Review No. (80)], and the written informed consents of all subjects were also acquired.

### Isolation of CAFs and exosomes

GC tissue blocks were cut into 1 mm<sup>3</sup> and then treated with 0.1% collagenase III (GC19590, Glpbio, China) and hyaluronidase (125 units/mL; GC19790, Glpbio, China) at 37°C overnight. Undissociated tissues were filtered, and stromal cells were centrifuged for 5 minutes (min) to obtain CAFs. The supernatants were resuspended in Dulbecco's Modified Eagle Medium (DMEM; D0819, Sigma-Aldrich, USA) containing 10% fetal bovine serum (FBS) (C0227, Beyotime, China), and then incubated at 37°C with 5% CO<sub>2</sub>. Normal fibroblasts (NFs) were isolated using paracancerous tissue as described above [20].

The isolation of exosomes from serum and cells was conducted using the differential centrifugation method mentioned in a previous literature [20]. Briefly, after removal of cells and other debris, the supernatant was centrifuged at 10,000 × g for 30 min at 4°C. After the pellet was suspended in serum-free DMEM, centrifugation was performed again at high speed for 70 min. After discarding the supernatant, we collected the exosomes. Transmission electron microscopy (TEM) was

then employed to observe the morphology of serum exosomes or cellular exosomes.

### **Cells, transfection and co-culture system**

GC cells AGS (CRL-1739, American Type Culture Collection, USA) and HGC-27 (RCB0500, RIKEN BioResource Research Center, Japan) were cultured in DMEM blended with 10% FBS at 37°C with 5% CO<sub>2</sub>.

MiR-29b-1-5p inhibitor (miR20004514-1-5) and inhibitor control (miR2N0000002-1-5) were bought from RIBOBIO (China). MiR-29b-1-5p mimic (M; miR10004514-1-5) and mimic control (MC; miR1N0000002-1-5) were also ordered from RIBOBIO to perform dual-luciferase reporter assay. Short hairpin RNA (shRNA) targeting VSIG1 (shVSIG1) and shNC (C01001) were obtained from GenePharma (China) to achieve silencing of VSIG1 or act as the control in GC cells. Lipofectamine 3000 reagent (L3000015, Thermo Fisher, USA) was utilized for cell transfection.

To investigate the effect of CAF-derived exosomal miR-29b-1-5p on GC cells, the following groupings and manipulations were performed. In control group, AGS or HGC-27 cells were co-cultured with CAF-derived exosomes. In IC group, CAFs transfected with inhibitor control were extracted into exosomes and then exosomes were co-cultured with AGS or HGC-27 cells. In I Group, exosomes were derived from CAFs transfected with miR-29b-1-5p inhibitor and subsequently co-cultured with AGS or HGC-27 cells. In MC or M group, exosomes were derived from CAFs transfected with mimic control or miR-29b-1-5p mimic and subsequently co-cultured with AGS and HGC-27 cells.

To investigate whether CAF-derived exosomal miR-29b-1-5p targets VSIG1 to regulate GC cell progression, the groupings were as follows: Control group (AGS or HGC-27 cells were co-cultured with CAF-derived exosomes); IC+shNC group (AGS or HGC-27 cells were co-cultured with CAF-derived exosomes transfected with miR-29b-1-5p inhibitor control and shNC); I +shNC group (AGS or HGC-27 cells were co-cultured with CAF-derived exosomes undergoing transfection of miR-29b-1-5p inhibitor and shNC);

and I+shVSIG1 group (AGS or HGC-27 cells were co-cultured with CAF-derived exosomes transfected with miR-29b-1-5p inhibitor and shVSIG1).

### **Quantitative real-time polymerase chain reaction (Qrt-PCR)**

GC tissues, serums, cells and transplanted tumor tissue were collected to isolate total RNAs using Trizol reagent (93289, Sigma-Aldrich, USA). After measurement of the RNA quality, total RNAs were synthesized to cDNA with reverse transcription kits (4304134 for the cDNA synthesis via mRNA, 4366597 for the cDNA synthesis via miRNA; Invitrogen, USA). For real-time PCR assay, SYBR Green Mix (FSSGMMRO, Roche, Switzerland) with LightCycler System (Roche Diagnostics, Switzerland) was utilized. The fold changes were calculated using the comparative  $2^{-\Delta\Delta CT}$  method, and standardized by  $\beta$ -actin or U6. Primer sequences are as follows (5'-3'). MiR-29b-1-5p: GGTTTAGAGTCGATCCAGTGCAA, TATCCAGTGCCTGTCGTGGA; U6: CTCGCTTC GGCAGCACA, AACGCTTCACGAATTTGCGT; VSIG1: ATGGTGTTCGCATTTTGGAAAGG, ACG TTCACGAAACCGTCTGG; zonula occluden-1 (ZO-1): CAACATACAGTGACGCTTCACA, CACTATTGACGTTTCCCCACTC;  $\beta$ -actin: CATGTACGTTGCTATCCAGGC, CTCCTTAATGTCACGCACGAT.

### **Immunohistochemistry**

4- $\mu$ m-thick histological sections were taken from paraffin-embedded GC tissues or paracancerous tissues or xenograft tumor samples for immunohistochemical staining to assess VM formation. After routine deparaffinization and hydration, sections were subjected to heat induction in citrate buffer (005000, Thermo Fisher, USA) for antigen retrieval. Next, sections were incubated with anti-CD34 antibody (#3569, 1/50, Cell Signaling Technology (CST), USA) at 4°C overnight. Subsequently, the corresponding secondary antibody (#8125, CST, USA) was applied to incubate the sections at room temperature for 30 min. Later, sections were then stained by Periodic Acid-Schiff (PAS) Staining Kit (C0142, Beyotime, China) according to the instructions.

Finally, VM structure was observed under a microscope (DP27, Olympus, Japan) (magnification  $\times 100$ ).

### **Western blot**

Western blot was applied to measure CAF markers, exosomal markers, and epithelial-mesenchymal transition (EMT)- or VM-related proteins. GC samples, cells as well as transplanted tumor tissues were obtained to collect protein samples using lysis buffer (R0010, Solarbio, China). Subsequently, proteins were separated by sodium dodecyl sulfate polyacrylamide gel electrophoresis, and then blotted onto polyvinylidene difluoride membranes (ISEQ00010, IPVH00010; Millipore, USA). Then, the membranes were blocked in 5% fat-free milk for about 1 hour (h), followed by co-incubation with primary antibodies at 4°C overnight and horseradish peroxidase (HRP)-conjugated secondary antibodies for 1 h. Afterwards, the enhanced chemiluminescence kit (WP20005, Invitrogen, USA) was employed to visualize the protein blots. The primary antibodies used in this study include those against TSG101 (ab125011, 45kDa, 1/1000, Abcam), HSP70 (ab2787, 70kDa, 1/1000, Abcam), CD63 (ab216130, 26kDa, 1/2000, Abcam),  $\alpha$ -SMA (ab5694, 2  $\mu$ g/mL, 42kDa, Abcam), FAP (ab235300, 58kDa, 1/2000, Abcam), FSP1 (1/1000, ab197896, 12kDa, Abcam), VSIG1 (-14145-1-AP, 65kDa, 1/2000, Proteintech), ZO-1 (ab276131, 195kDa, 1/1000, Abcam), VE-Cadherin (ab33168, 1  $\mu$ g/mL, 115kDa, Abcam), E-cadherin (ab231303, 97kDa, 1  $\mu$ g/mL, Abcam), N-cadherin (ab18203, 130kDa, 1/1000, Abcam), Vimentin (ab8978, 53kDa, 1/1000, Abcam) and  $\beta$ -actin (ab8226, 42kDa, 1  $\mu$ g/mL, Abcam). Here, the secondary antibodies are Goat Anti-Rabbit IgG (ab97051, diluted 1/5000, Abcam, UK) and Goat Anti-Mouse IgG (ab205719, diluted 1/5000, Abcam, UK).

### **PKH-26 labeling**

Exosomes were extracted from CAFs and subsequently labeled with PKH-26 (MIDI26, Sigma-Aldrich, USA). Simply put,  $1 \times 10^4$  GC cells were

seeded in DMEM with 10% exosome-free FBS and then incubated with purified PKH26-labeled exosomes. After 12-h incubation, exosome uptake of GC cells was visualized and recorded by a fluorescence microscope (BD-YG3001, Shenzhen Boshida Optical Instrument Co., Ltd, China).

### **Cell counting kit-8 (CCK-8) assay**

After transfection for 24, 48, or 72 h, CCK-8 kit (40203ES60\*, YEASEN, China) was used to analyze the effect of CAF-derived exosomal miR-29b-1-5p on GC cell viability. Briefly, the GC cells were mixed with CCK-8 solution (10  $\mu$ L) and cultivated for 3 h. Thereafter, optical density (OD) value at a wavelength of 450 nm was assessed using a microplate reader (Varioskan LUX, Thermo Fisher, USA).

### **Flow cytometry**

The apoptosis assay was carried out using Annexin V-FITC Apoptosis Detection Kit (CA1020, Solarbio, China). In a nutshell, AGS or HGC-27 cells at  $1 \times 10^6$  cells/mL were resuspended in Binding Buffer (1 $\times$ ), mixed with 5  $\mu$ L Annexin V/FITC for 5 min, and stained with propidium iodide (PI) reagent. Subsequently, a flow cytometer (A24860, Thermo Fisher, USA) was used to assess the cell apoptosis.

### **Wound healing assay**

For migration assay, GC cells AGS or HGC-27 ( $1 \times 10^5$  cells/well) were grown in a 6-well plate. A sterile pipette tip was utilized to create wounds on the monolayers after cells were completely confluent. Then, cells were additionally cultured in DMEM without FBS for 48 h, and observed by a microscope ( $\times 100$ ).

### **Transwell assay**

For detect invasion rate, GC cells AGS or HGC-27 in serum-free DMEM were added to the upper Transwell chamber with 8- $\mu$ m pore (3422, Corning, USA) which was pre-coated with Matrigel matrix (354234, Corning, Inc.). Additionally, complete medium containing 10% FBS was added into the lower chamber as the



chemoattractant. After 48-h culture, cells were fixed with 4% paraformaldehyde (P1110, Solarbio, China) and stained using crystal violet (G1063, Solarbio, China) for 20 min, followed by observation under a microscope at a magnification of  $\times 250$ .

### **Tube formation assay**

To investigate the effect of miR-29b-1-5p/VSIG1 on VM formation in GC cells, tube formation experiments were performed. AGS or HGC-27 cells were seeded in 96-well plates ( $3 \times 10^4$  cells/well) pre-coated with Matrigel and cultured in FBS-free DMEM. 8 h later, images were captured using an inverted microscope, and VMs were analyzed using the ImageJ software (National Institutes of Health, USA).

### **Bioinformatics analysis and dual-luciferase reporter assay**

TargetScan ([http://www.targetscan.org/vert\\_72/](http://www.targetscan.org/vert_72/)) was applied to analyze the binding sites between VSIG1 and miR-29b-1-5p, which was verified by dual-luciferase reporter assay.

For dual-luciferase reporter assay, the putative miR-29b-1-5p complementary sites in VSIG1 gene were inserted into pmirGLO vector (BR377, Fenghuishengwu, China) as VSIG1-WT group, while the sequence of the miR-29b-1-5p binding sites in VSIG1 was mutated and then recombined into pmirGLO vector as VSIG1-MUT group. Co-transfection of VSIG1-MUT or VSIG1-WT with miR-29b-1-5p mimic into HEK-293 cells was accomplished under the help of Lipofectamine 3000 transfection reagent, with miR-29b-1-5p mimic control as the negative control. Dual-luciferase Reporter Assay System (E1960, Promega Corporation, USA) was applied to analyze luciferase activity.

### **RNA immunoprecipitation (RIP) experiments**

To verify the binding relationship between VSIG1 and miR-29b-1-5p, RIP experiments were performed using the Megna RIP RNA-binding Protein Immunoprecipitation Kit (17-700; Millipore, Burlington, MA, USA) according to

the manufacturer's instructions. AGS and HGC-27 cells were lysed using RIP lysis buffer, and then the whole-cell lysates were incubated with anti-VSIG1 or anti-IgG antibodies at 4°C overnight, followed by the incubation with protein A magnetic beads at 4°C for 4 h. The co-precipitated RNAs were isolated to quantify the expression levels of miR-29b-1-5p by RT-qPCR. To demonstrate that miR-29b-1-5p specifically bound to VSIG1, total RNA (input controls) and normal rabbit IgG controls were simultaneously assessed.

### **Co-immunoprecipitation (Co-IP) assay**

The interaction between VSIG1 and ZO-1 in GC cells was determined using the co-immunoprecipitation kit (88804) from Thermo Scientific (USA). Total proteins were extracted from AGS cells using IP lysis/wash buffer and incubated with antibody against IgG or VSIG1 (sc-52,520, Santa Cruz, USA) or ZO-1 (1/100) at 4°C overnight, and the appropriate amount of protein was extracted as Input group. Subsequently, Pierce Protein A/G Magnetic Beads were added and incubated for 2 h. The protein-magnetic bead complexes were then eluted to collect the supernatant for Western blot analysis.

### **Xenograft tumor assay**

A total of 20 BALB/c mice (5 weeks old; catalog no. 401) were purchased from Charles River (China), and housed in an SPF grade animal room with regular feeding and drinking. Next, equal amounts of HGC27 cells ( $1 \times 10^6$ ) were orthotopically implanted in nude mice. Then, mice were randomly divided into IC group or I group ( $n = 10$ ). Specifically, mice were injected with 100  $\mu$ L of exosomes derived from CAFs transfected with inhibitor control or miR-129b-1-5p inhibitor into the tail vein once a week for continuous five weeks. Afterwards, tumor volumes were measured on days 3, 10, 15, 20, 25, 30 and 35, and calculated using the formula: tumor volume = (width)<sup>2</sup>  $\times$  (length)/2. On the last measurement day, mice were euthanized by cervical dislocation after anesthesia with 3% isoflurane (Wuhan piluofu Biotechnology Co., Ltd,

China). Then, the tumors were removed, weighted, photographed and stored for subsequent experiments.

### Statistical analysis

Measurement data were expressed as mean  $\pm$  standard deviation. A paired *t*-test was used to compare the difference between adjacent tissues and cancer tissue (not metastasized) or cancer tissue (metastasized). Comparisons between two groups were conducted using independent samples *t* test, whilst one-way analysis of variance (ANOVA) was performed for comparison among multiple groups. All statistical analyses were accomplished using Graphpad 8.0 software (GraphPad Software, USA), and  $P < 0.05$  was indicated to be statistically significant.

## Results

### VM structure and highly expressed miR-29b-1-5p level were presented in GC tissues

MiR-29b-1-5p level was analyzed in collected clinical samples. The results showed that the expression of miR-29b-1-5p in GC tissues was appreciably higher than that in paracancerous tissues, and was also markedly higher in metastatic GC tissues than in non-metastatic GC tissues ( $P < 0.001$ , Figure 1a). Subsequently, we examined miR-29b-1-5p level in serum. Similarly, miR-29b-1-5p expression was found to be abnormally elevated in the serum of GC patients. In addition, miR-29b-1-5p expression was also obviously higher in the serum of metastatic GC patients than that in non-metastatic patients ( $P < 0.001$ , Figure 1b). Through immunohistochemistry staining, we observed that VM structure was visualized in GC tissues, and metastatic GC tissues had more VM than non-metastatic GC tissues (Figure 1c).

### Identification of CAFs and exosomes

We extracted CAFs and identified them by Western blot. Compared with NFs, CAFs contained higher expression levels of  $\alpha$ -SMA, FAP and FSP1 ( $P < 0.05$ , Figure 2a). Through TEM, we observed that

serum exosomes and cellular exosomes were successfully extracted. Besides, the results of Western blot showed high expressions of TSG101, HSP70 and CD63 in exosomes (Figure 2b,c). Subsequently, we discovered that the expression of miR-29b-1-5p in serum exosomes of GC patients was starkly higher than that of healthy controls ( $P < 0.001$ , Figure 2d). Also, miR-29b-1-5p expression was significantly higher in the serum exosomes of metastatic GC patients than that in non-metastatic patients ( $P < 0.001$ , Figure 2d). Meanwhile, the expression of miR-29b-1-5p was also conspicuously higher in CAF-derived exosomes than that in NF-derived exosomes ( $P < 0.05$ , Figure 2d). In addition, we explored whether CAF-derived exosomal miR-29b-1-5p can be taken up by GC cells. The red fluorescent dye PKH26 was used to label miR-29b-1-5p-containing exosomes (miR-29b-1-5p Exos) isolated from CAFs. PKH-26 labeling showed that CAF-derived exosomal miR-29b-1-5p was internalized by AGS cells (Figure 2e). These findings revealed that these miR-29b-1-5p-containing exosomes were transferred from CAFs to GC cells. Additionally, the results indicated that the expression of miR-29b-1-5p is higher in CAF than that in NF, AGS and HGC-27 cells (supplementary Fig. S1).

### Downregulation of CAF-derived exosomal miR-29b-1-5p regulated the biological function of GC cells

The level of miR-29b-1-5p in GC cells (AGS and HGC-27) was also inhibited after co-culture with exosomes extracted from CAFs transfected with miR-29b-1-5p inhibitor ( $P < 0.001$ , Figure 3a,b). Compared with IC group, I group presented a decrease in GC cell viability and an increase in GC cell apoptosis ( $P < 0.01$ , Figure 3c-f). Besides, we found that downregulating miR-29b-1-5p level in CAFs reduced GC cell migration and invasion ( $P < 0.01$ , Figure 4a-d). Not surprisingly, VM formation was distinctly lower in I group than that in IC group ( $P < 0.001$ , Figure 5a,b). VSIG1 could bind to ZO-1, which has been shown to be involved in tumor metastasis [21,22]. Here, we found that downregulation of CAF-derived exosomal miR-29b-1-5p could elevate VSIG1 and ZO-1 protein levels in

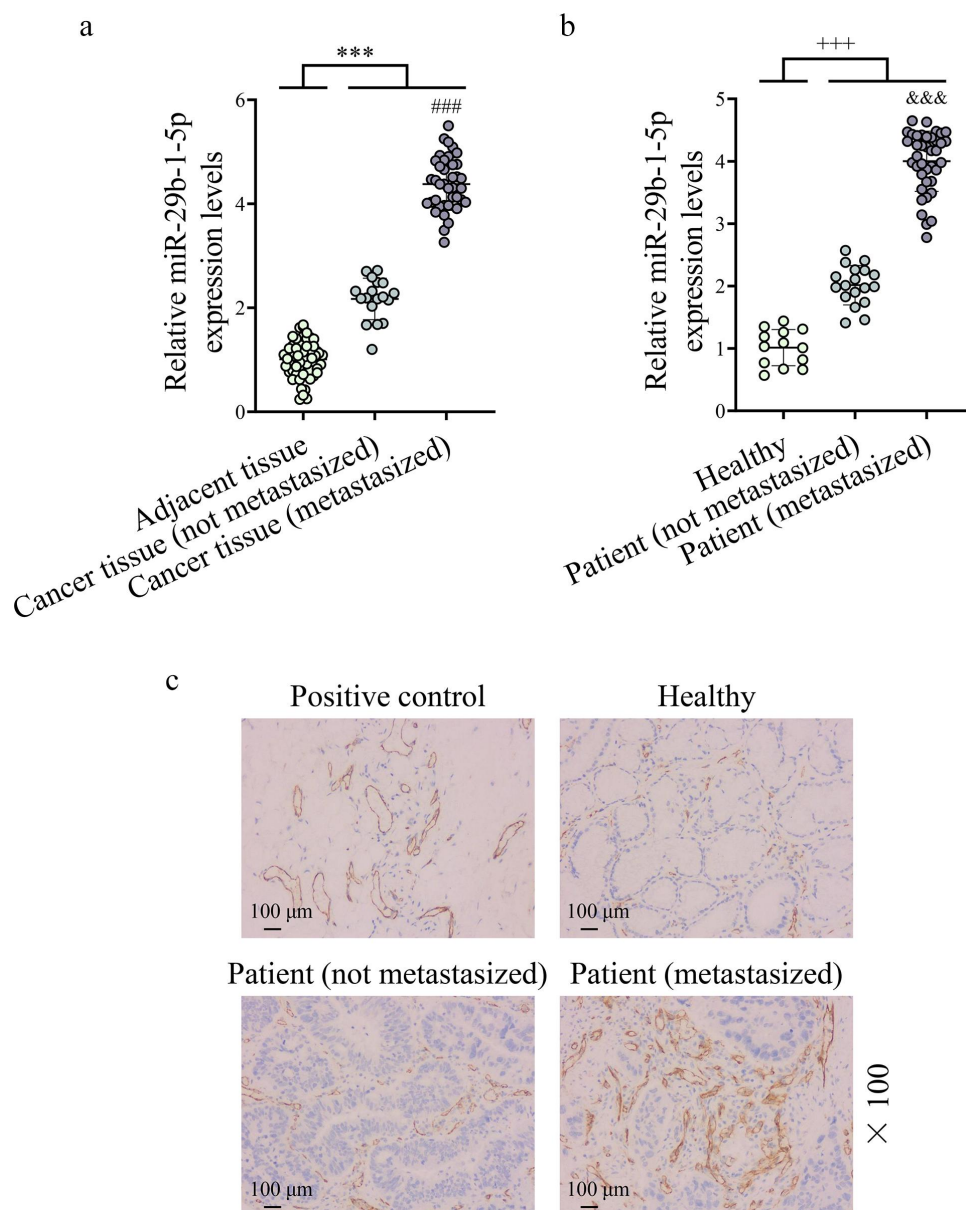


**Figure 1.** Vasculogenic mimicry (VM) structures appear in gastric cancer (GC) tissues and show high levels of miR-29b-1-5p. (a) the expression of miR-29b-1-5p in GC tissues [non-metastasized tissues ( $n = 18$ ) and metastasized tissues ( $n = 39$ )] and adjacent tissues (para-cancerous tissues,  $n = 57$ ) was detected by quantitative real-time polymerase chain reaction (Qrt-PCR) assay. A paired t-test was used to compare the difference between adjacent tissues and cancer tissue (not metastasized) or cancer tissue (metastasized); independent sample t test was used to compare the difference between cancer tissue (not metastasized) group and cancer tissue (metastasized) group. (b) Qrt-PCR assay was also used to detect the expression of miR-29b-1-5p in the serum of GC patients [non-metastasized GC patients ( $n = 18$ ) and metastasized GC patients ( $n = 39$ )] and normal volunteers ( $n = 13$ ). One-way analysis of variance (ANOVA) was performed for comparison among multiple groups. (c) Immunohistochemical staining (PAS, CD34 double staining) was performed to analyze VM structure in normal and GC tissues. Normal gastric tissues ( $CD34^+/PAS^+$ ) were set as the positive control (scale bar, 100  $\mu$ m).

Note: \*\*\* $P < 0.001$  vs. Adjacent tissue; ### $P < 0.001$  vs. Cancer tissue (non- metastasized); +++ $P < 0.001$  vs. Healthy; &&& $P < 0.001$  vs. Patient (non- metastasized).

GC cells ( $P < 0.05$ , Figure 5c,d). In addition, the level of miR-29b-1-5p in GC cells (AGS and HGC-27) was also elevated after co-culture with exosomes extracted from CAFs transfected with miR-29b-1-5p mimic ( $P < 0.001$ , Supplementary

Fig. S2A-B). miR-29b-1-5p overexpression also promoted GC cell viability ( $P < 0.05$ , Supplementary Fig. S2C-D), migration ( $P < 0.001$ , Supplementary Fig. S3A-B) and invasion ( $P < 0.01$ , Supplementary Fig. S3C-D).

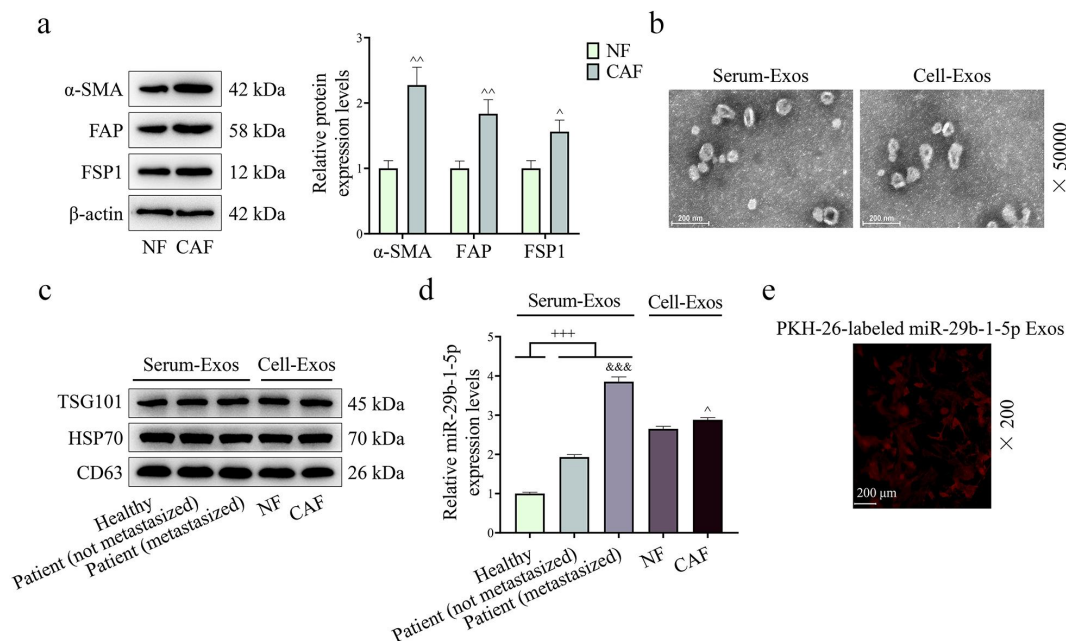


**Figure 2.** Extraction and identification of cancer associated fibroblasts (CAFs) and exosomes. (a) the protein expressions of  $\alpha$ -SMA, FAP and FSP1 were determined by Western blot.  $n = 3$ . (b) the morphology of exosomes was observed by transmission electron microscopy (TEM). (c) Exosome-related markers TSG101, HSP70 and CD63 were also determined by Western blot. (d) the expression of miR-29b-1-5p in exosomes from serum of GC patients [non-metastasized GC patients ( $n = 18$ ) and metastasized GC patients ( $n = 39$ )] and normal volunteers ( $n = 13$ ), NF and CAF was quantified by Qrt-PCR. (e) PKH-26 labeling was used to analyze the uptake of exosome in AGS cells.

Note:  $+++P < 0.001$  vs. Healthy;  $\\\&\&P < 0.001$  vs. Patient (non-metastasized).  $^{\wedge}P < 0.05$ ,  $^{\wedge\wedge}P < 0.01$  vs. Normal fibroblast (NF).

### CAF-derived exosomal miR-29b-1-5p may affect GC migration, invasion and VM formation by regulating VSIG1/ZO-1

The binding sites of miR-29b-1-5p to VSIG1 were shown in Figure 6a. Dual-luciferase reporter and RIP experiments validated that miR-29b-1-5p bound to VSIG1 ( $P < 0.001$ , Figure 6b-d). Next, we demonstrated the low expressions of VSIG1 and ZO-1 in GC tissues ( $P < 0.001$ , Figure 6e,f). Subsequently, miR-29b-1-5p inhibitor with or without shVSIG1 were transfected into CAFs for the rescue experiments. The results revealed that the downregulation of CAF-derived exosomal miR-29b-1-5p decreased the level of miR-29b-1-5p yet increased VSIG1 expression, and could reverse the shVSIG1-induced downregulation of VSIG1. However, shVSIG1 had no obvious effect on the level of miR-29b-1-5p ( $P > 0.05$ , Figure 7a-d).

Functional experiments uncovered that shVSIG1, contrary to miR-29b-1-5p inhibitor, increased the viability, migration, invasion and VM formation, but inhibited apoptosis of GC

cells, and partially offset the effect of miR-29b-1-5p inhibitor on the biological function of GC cell ( $P < 0.05$ , Figure 7e-j, Figure 8A-B and Figure 9A-H). Mechanistically, we examined VM- and migration-related markers, and found that miR-29b-1-5p inhibitor elevated ZO-1 and E-cadherin levels, but lessened VE-cadherin, N-cadherin, and Vimentin levels ( $P < 0.05$ , Figure 10a-k). ShVSIG1 had the opposite effect on the above proteins and partially neutralized the regulatory effect of miR-29b-1-5p inhibitor ( $P < 0.05$ , Figure 10a-k). Furthermore, Co-IP assay verified that VSIG1 binds to ZO-1 (Figure 10l).

### Downregulation of CAF-derived exosomal miR-29b-1-5p inhibited GC growth, VM formation and EMT process *in vivo*

As shown in Figure 11(a-d), downregulation of miR-29b-1-5p in CAFs was able to inhibit GC tumor growth ( $P < 0.01$ ). Besides, qRT-PCR assay showed that the level of miR-29b-1-5p in tumor tissue was downregulated in I group ( $P < 0.001$ ,



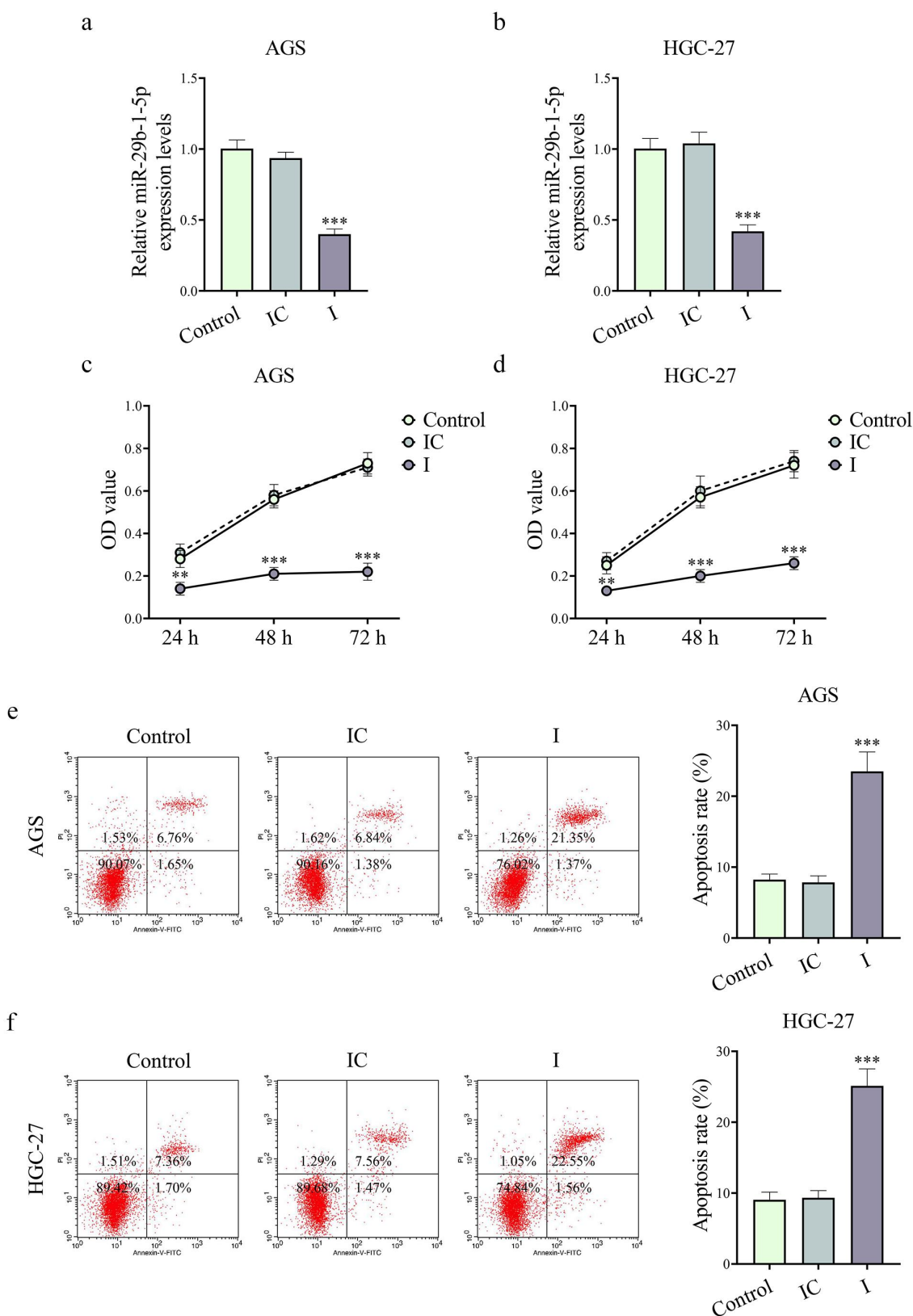


**Figure 3.** Downregulation of CAF-derived exosomal miR-29b-1-5p inhibited the viability while accelerating the apoptosis of GC cells. (a-b) the effect of CAF-derived exosomal miR-29b-1-5p inhibitor on miR-29b-1-5p level in AGS and HGC-27 cells was evaluated by Qrt-PCR. (c-d) the effect of downregulated miR-29b-1-5p on GC cell viability was assessed by cell counting kit-8 (CCK-8) assay. (e-f) Downregulation of miR-29b-1-5p accelerated the apoptosis of AGS and HGC-27 cells as determined by flow cytometry.  $n = 3$ . Note: \*\* $P < 0.01$ , \*\*\* $P < 0.001$  vs. inhibitor control (IC).

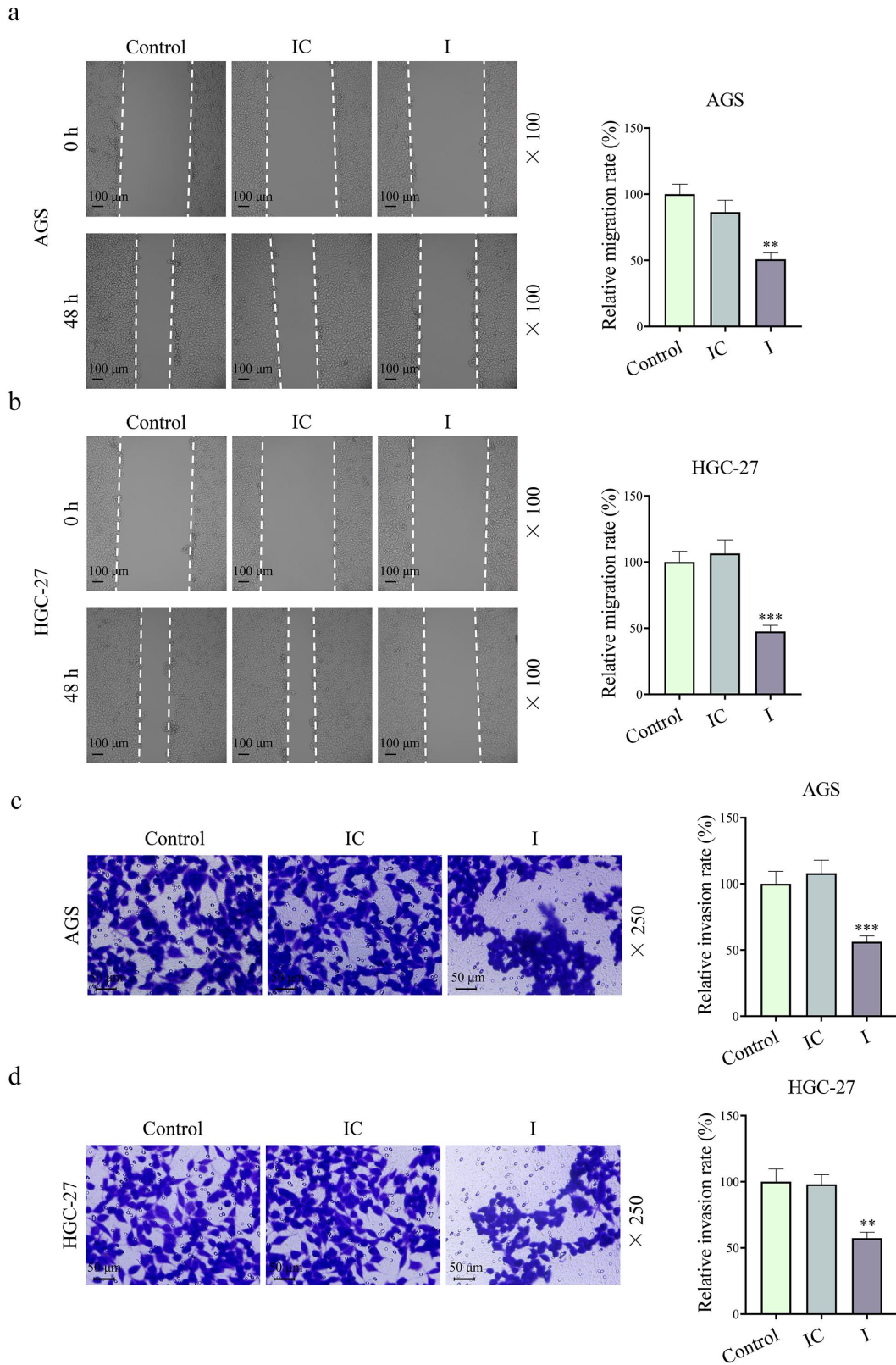


**Figure 4.** Downregulation of CAF-derived exosomal miR-29b-1-5p repressed GC cell migration and invasion. (a-b) Wound healing assay was applied to examine the relative migration rates of control GC cells, or GC cells co-cultured with miR-29b-1-5p inhibitor/inhibitor control-transfected exosomes for 48 h. (c-d) Invasion rate of GC cells was assessed using Transwell assays.  $n = 3$ .

Note: \*\* $P < 0.01$ , \*\*\* $P < 0.001$  vs. IC.

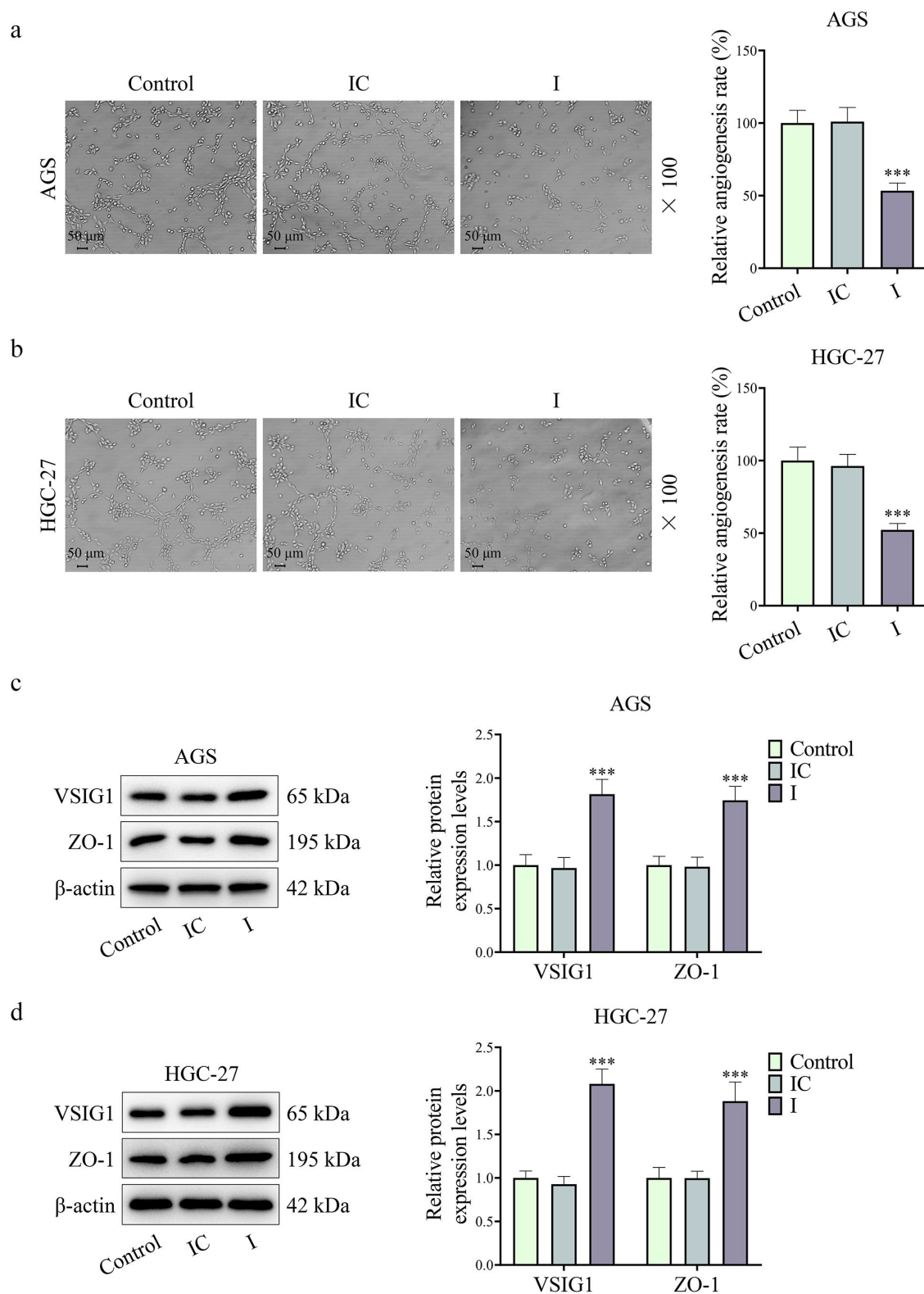


**Figure 5.** Downregulation of CAF-derived exosomal miR-29b-1-5p reduced VM formation yet increased VSIG1 and ZO-1 expressions. (a-b) the tubule formation assay was applied to assess the effect of miR-29b-1-5p downregulation on VM in GC cells. (c-d) the protein expressions of VSIG1 and ZO-1 were both increased after miR-29b-1-5p expression was downregulated, as determined by Western blot.  $n = 3$ .

Note: \* $P < 0.05$ , \*\* $P < 0.01$ , \*\*\* $P < 0.001$  vs. IC.

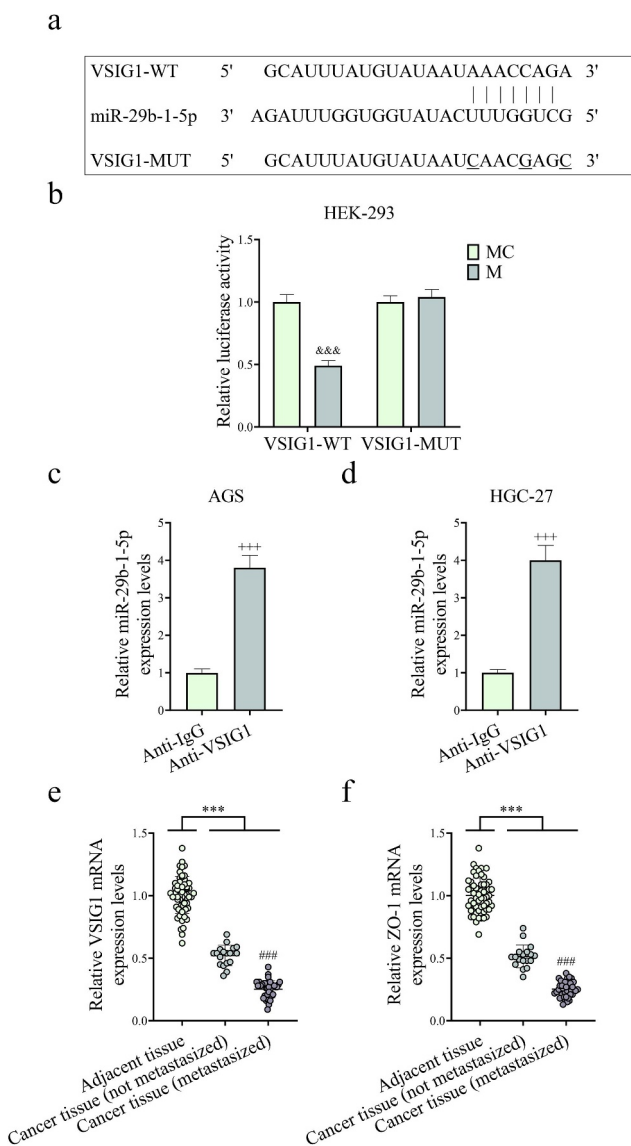


**Figure 6.** MiR-29b-1-5p may target and regulate VSIG1/ZO-1. (a) TargetScan was employed to predict the targeted binding sequence of miR-29b-1-5p to VSIG1. (b-d) Dual-luciferase reporter and RNA immunoprecipitation (RIP) experiments were used to determine the binding of miR-29b-1-5p to VSIG1.  $n = 3$ . (e-f) the expressions of VSIG1 and ZO-1 in GC non-metastatic or metastatic tissues [non-metastasized tissues ( $n = 18$ ) and metastasized tissues ( $n = 39$ )] and adjacent tissues (para-cancerous tissue,  $n = 57$ ) were detected by Qrt-PCR.  $***P < 0.001$  vs. mimic control (MC).

Note:  $***P < 0.001$  vs. Adjacent tissue.

Figure 11e). Meanwhile, fewer VM structure was observed in I group than that in IC group (Figure 11f). In addition, downregulation of miR-29b-1-5p decreased the expression levels of endothelial marker (VE-Cadherin) and mesenchymal markers (N-cadherin, and Vimentin) in tumor tissues, but increased levels of VSIG1, ZO-1, and

epithelial cell marker (E-cadherin), which were consistent with the *in vitro* results ( $P < 0.05$ , Figure 11g). These findings indicated that down-regulation of CAF-derived exosomal miR-29b-1-5p hindered GC growth, VM formation, and EMT process via the VSIG1/ZO-1 axis *in vivo*.

## Discussion

CAFs play an important role in the malignant progression of tumors and participate in the proliferation, metastasis and angiogenesis of tumor cells [9,20]. MiRNAs not only affect the biological processes in tumor cells, but also regulate tumor progression by being abnormally expressed in CAFs and acting on tumor cells through exosomes [23,24]. Here, our study found that CAF-derived exosomal miR-29b-1-5p inhibitor weakened the viability, VM formation, migration and invasion, but promoted the apoptosis of GC cells by targeting the VSIG1/ZO-1 axis.

Initially, our study found that miR-29b-1-5p was abnormally highly expressed in GC tissues and serum samples and, importantly, even higher in metastatic GC patients. This suggests that abnormal expression of miR-29b-1-5p is involved in the process of GC metastasis. At this stage, the functional research of miR-29b-1-5p is still very limited, but its high expression has been proved in multiple GC studies [25,26], which further proves the correctness of the results in this study. Conversely, miR-29b-1-5p acts as a tumor suppressor gene in triple-negative breast cancer and colorectal cancer [27,28], which may be disease-specific. The abnormal expression of miR-29b-1-5p suggests that miR-29b-1-5p may be a driver gene of GC progression and serve as a potential diagnostic marker.

In recent years, researches on CAF-derived exosomal miRNAs have gradually increased [20,29,30]. For example, Wang et al. showed that CAF-derived exosomes containing miRNA-181d-5p promotes EMT by targeting the CDX2/HOXA5 axis in breast cancer [29]. Hu et al. found that exosomal miR-92a-3p secreted by CAFs enhances colorectal cancer metastasis and chemotherapy resistance [30]. The “shadow” of CAF-derived exosomal miRNAs has also been found in recent studies. For instance, GC Zhang et al. pointed



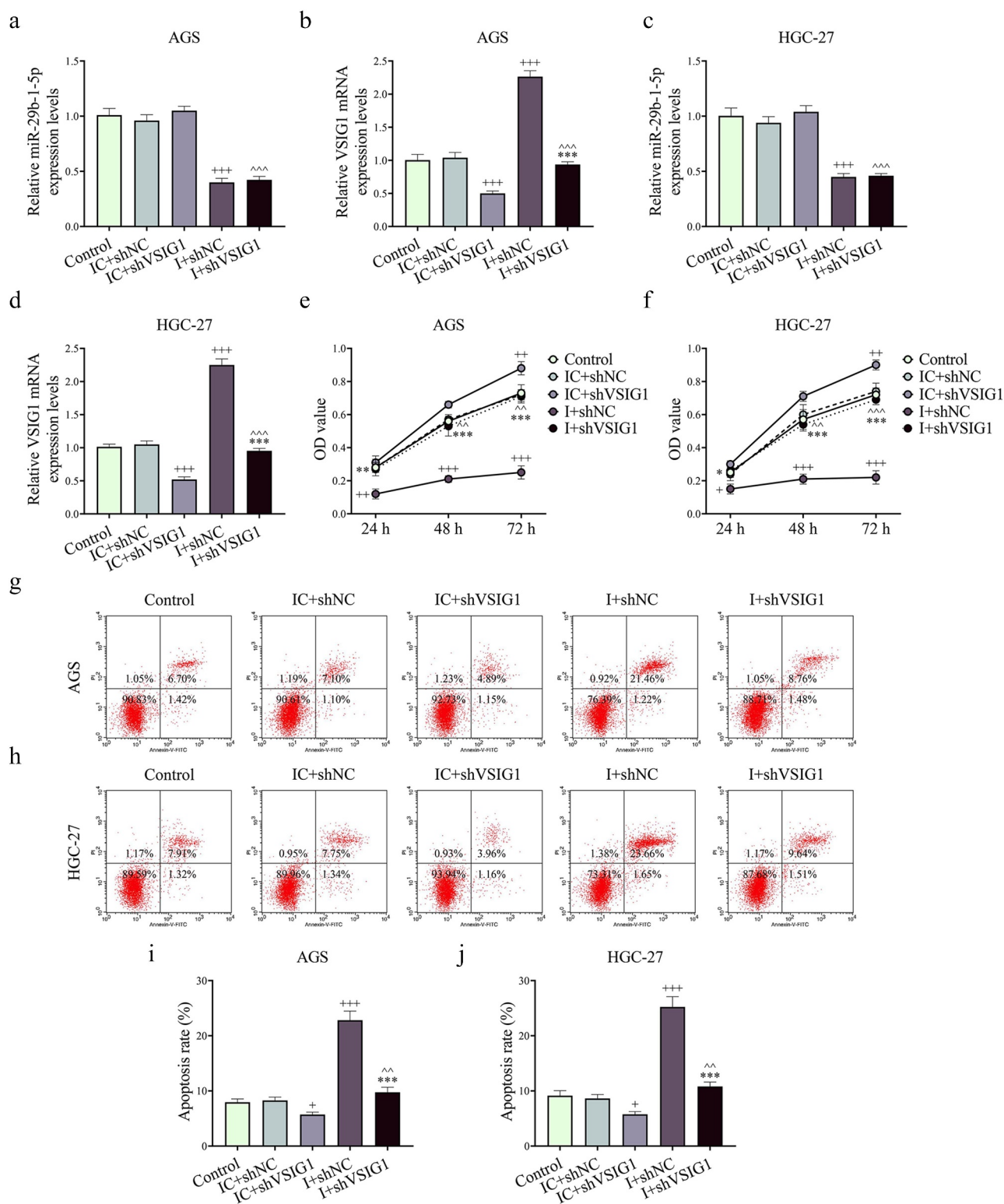


**Figure 7.** Silencing of CAF-derived exosomal VSIG1 reversed the effects of downregulated miR-29b-1-5p on the viability and apoptosis of GC cells. (a-d) ShVSIG1 or/and miR-29b-1-5p inhibitor was transfected into CAFs to extract exosomes which were subsequently co-cultured with GC cells. VSIG1 and miR-29b-1-5p levels in AGS and HGC-27 cells were quantified by Qrt-PCR assay. (e-f) Cell viability in control, IC+shNC, IC+shVSIG1, I+shNC and I+shVSIG1 groups was assessed by CCK-8 assay. (g-j) Cell apoptosis in each group was detected by flow cytometry.  $n = 3$ .  $^+P < 0.05$ ,  $^{++}P < 0.01$ ,  $^{+++}P < 0.001$  vs. IC+shNC;  $^*P < 0.05$ ,  $^{**}P < 0.01$ ,  $^{***}P < 0.001$  vs. I+shNC;  $^{\wedge}P < 0.01$ ,  $^{\wedge\wedge}P < 0.001$  vs. IC+shVSIG1.

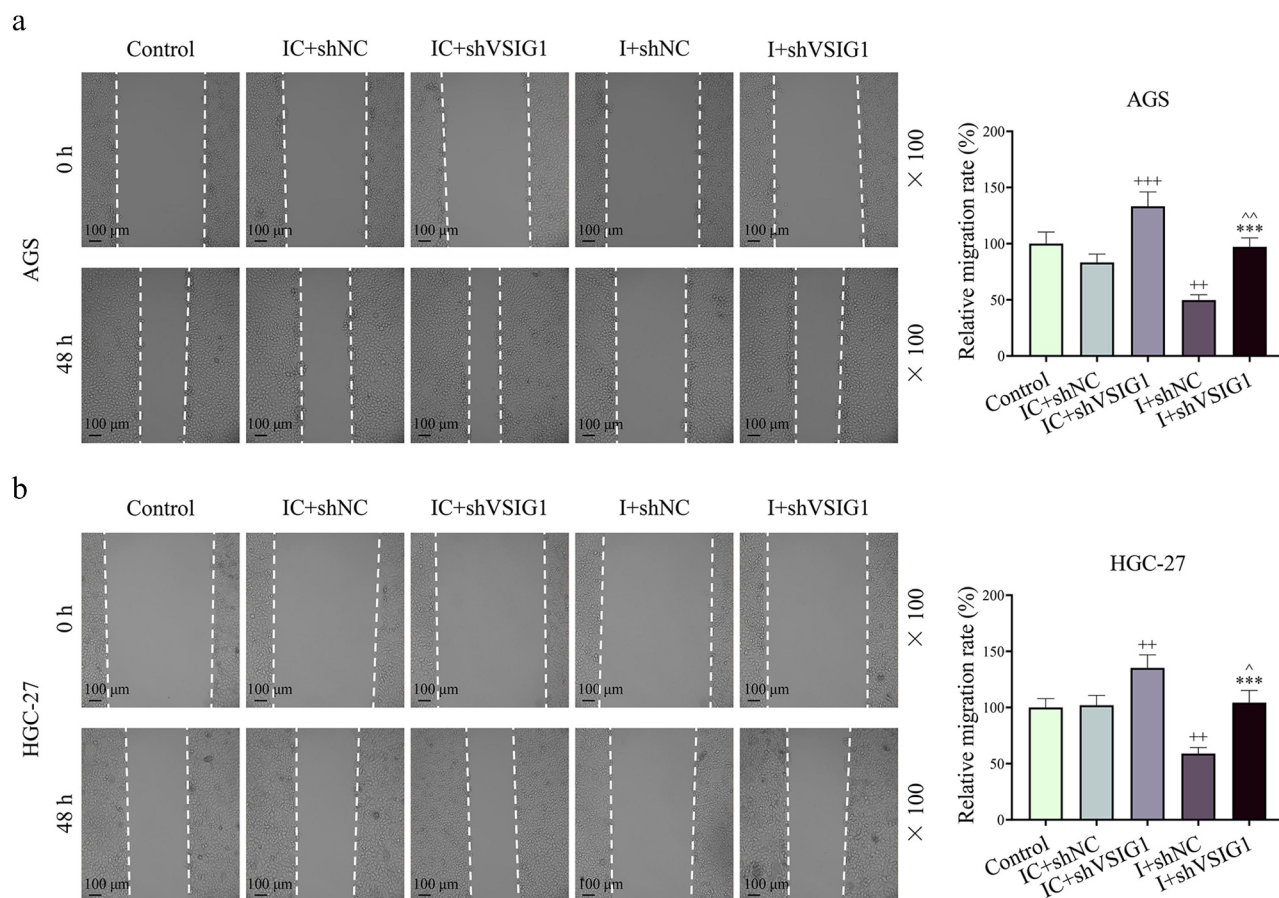


**Figure 8.** The effect of CAF-derived exosomal miR-29b-1-5p downregulation on GC cell migration was reversed by VSIG1 silencing. (a-b) Wound-healing assay was used to determine the relative migration rate of GC cells in control, IC+shNC, IC+shVSIG1, I+shNC, and I+shVSIG1 groups.  $n = 3$ .  $^{++}P < 0.01$ ,  $^{+++}P < 0.001$  vs. IC+shNC;  $^{***}P < 0.001$  vs. I+shNC;  $^{\wedge}P < 0.05$ ,  $^{\wedge\wedge}P < 0.01$  vs. IC+shVSIG1.

out that CAF-secreted exosomal miR-522 inhibits ferroptosis in GC cells by regulating ALOX15 and blocking lipid reactive oxygen species accumulation [20]. Our study revealed, for the first time, the role of CAF-derived exosomal miR-29b-1-5p in the VM formation and metastasis of GC cells, and discovered that downregulating the expression of miR-29b-1-5p in CAF may exert a certain inhibitory effect on the malignant progression of GC cells through exosomes. These findings suggest that CAF-derived exosomal miR-29b-1-5p may serve as a potential target for GC therapy.

In this study, VSIG1 was identified as a target gene regulated by miR-29b-1-5p. Silencing of VSIG1 in CAFs reversed the inhibitory effects of miR-29b-1-5p downregulation on VM formation and migration of GC cells. VSIG1, a cell adhesion protein, has long been shown to be lowly expressed in GC, and its loss of expression is associated with poor patients' prognosis [19]. In

addition, some scholars support the tumor suppressor function of VSIG1 in GC [31]. A recent study shows that the E-cadherin/VSIG1 complex can help inhibit tumor growth by limiting dedifferentiation of hepatocellular carcinoma [32]. VE-cadherin and ZO-1 are involved in the regulation of endothelial cell-cell adhesion and VM [33]. We also examined EMT and VM-related markers, signifying that VSIG1 silencing downregulates E-cadherin and ZO-1 levels, whereas up-regulating N-cadherin, VE-cadherin, and Vimentin levels. The effect of VSIG1 silencing could be reversed by CAF-derived exosomal miR-29b-1-5p inhibitor. A previous study has found that ZO-1 is a central structural protein in tight junctions and can interact with VSIG1 [22]. This result was also verified in our study. Interestingly, ZO-1 has shown the ability to prevent cancer cell metastasis in a variety of tumors [34–36]. Furthermore, it has been proposed that

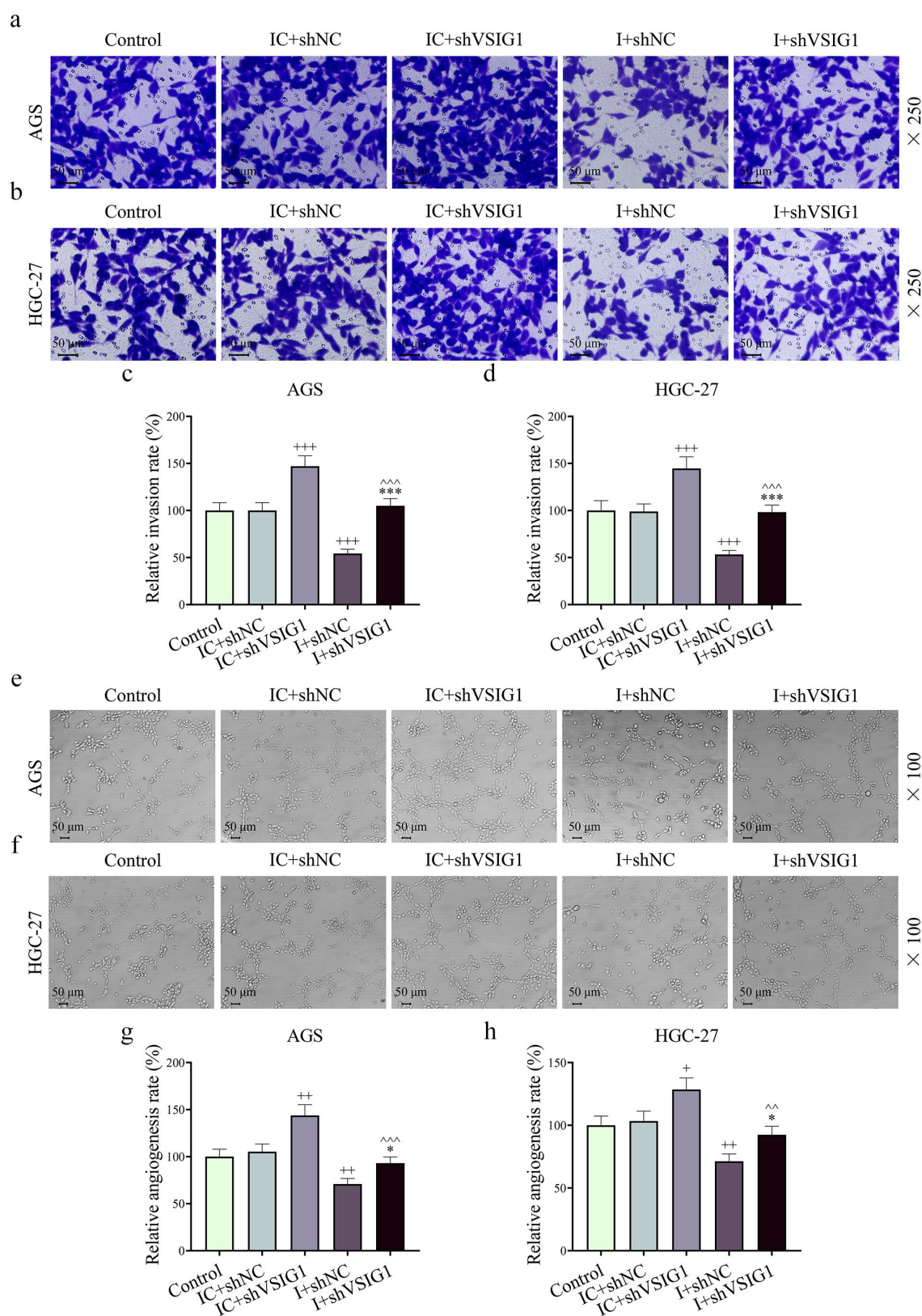


**Figure 9.** Both miR-29b-1-5p inhibitor and shVSIG1 of the CAF-derived exosome regulated GC cell migration and VM formation. (a-d) Transwell assay was conducted to evaluate the effects of CAF-derived exosomal miR-29b-1-5p inhibitor and shVSIG1 on GC cells. (e-h) the results of tube formation experiment demonstrated the effects of CAF-derived exosomal miR-29b-1-5p inhibitor and shVSIG1 on VM in GC cells.  $n=3$ .  $^*P<0.05$ ,  $^{++}P<0.01$ ,  $^{+++}P<0.001$  vs. IC+shNC;  $^*P<0.05$ ,  $^{***}P<0.001$  vs. I+shNC;  $^{^^}P<0.01$ ,  $^{^^^}P<0.001$  vs. IC+shVSIG1.



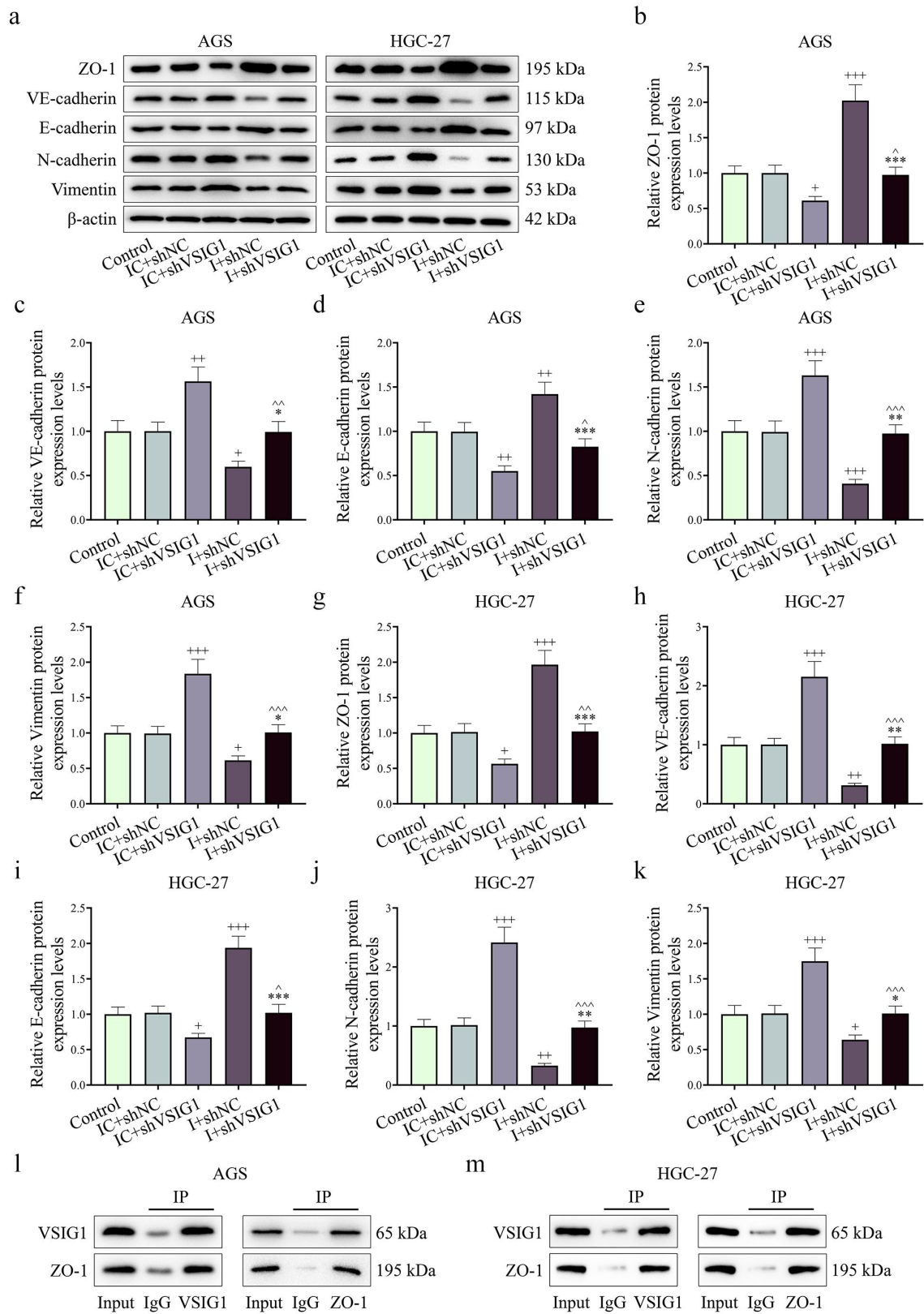


**Figure 10.** MiR-29b-1-5p may target VSIG1/ZO-1 to regulate metastasis- and VM-related protein expression. (a-k) the protein expressions of ZO-1, VE-cadherin, E-cadherin, N-cadherin and Vimentin in GC cells of each group were detected by Western blot. (L) Co-immunoprecipitation assay was employed to detect the interaction between VSIG1 and ZO-1.  $n = 3$ .  $^+P < 0.05$ ,  $^{++}P < 0.01$ ,  $^{+++}P < 0.001$  vs. IC+shNC;  $^*P < 0.05$ ,  $^{**}P < 0.01$ ,  $^{***}P < 0.001$  vs. I+shNC;  $^{\wedge}P < 0.05$ ,  $^{\wedge\wedge}P < 0.01$ ,  $^{\wedge\wedge\wedge}P < 0.001$  vs. IC+shVSIG1.



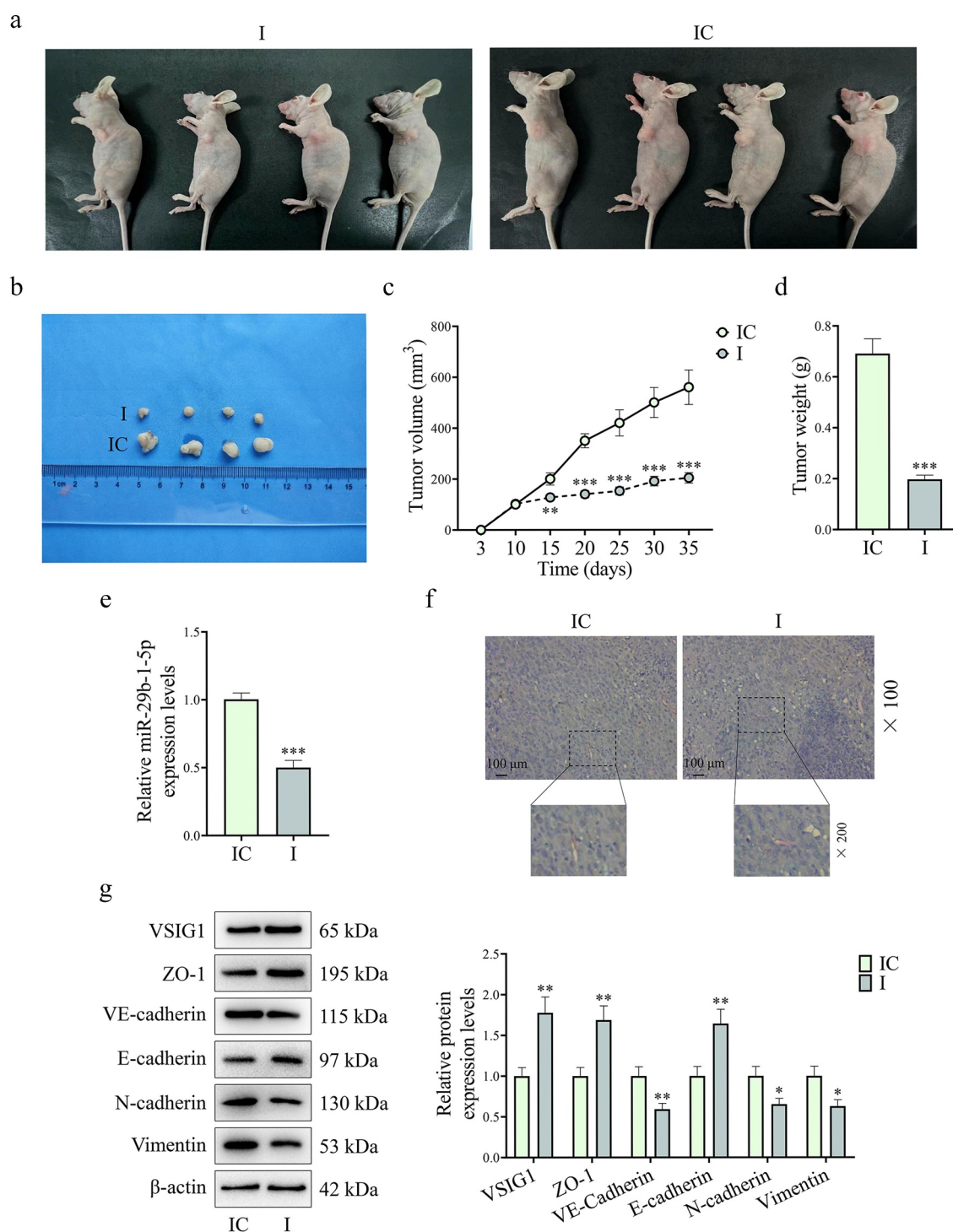


**Figure 11.** Downregulation of CAF-derived exosomal miR-29b-1-5p inhibited GC occurrence and metastasis in vivo. (a-d) BALB/c mice were orthotopically inoculated with HGC27 cells to construct a xenograft tumor model, and then injected with exosomes derived from CAFs transfected with miR-29b-1-5p inhibitor control or inhibitor through the tail vein to observe tumor growth. (e) MiR-29b-1-5p expression in mouse tumor tissues was quantified by Qrt-PCR assay. (f) VM (PAS positive staining without CD31 staining) in the tissues of mice in each group was detected by immunohistochemical staining. (g) Western blot was used to measure the expressions of metastasis- and VM-related proteins (VSIG1, ZO-1, VE-Cadherin, E-cadherin, N-cadherin and Vimentin).  $n = 10$  mice/group.

Note: \* $P < 0.05$ , \*\* $P < 0.01$ , \*\*\* $P < 0.001$  vs. IC.

hypoxic lung cancer-secreted exosomal miR-23a inhibits ZO-1, thereby enhancing vascular permeability and cancer transendothelial migration [37]. In line with the above information, we speculated and verified that VSIG1 regulated the malignant progression of GC cells by interacting with ZO-1. In addition, based on the xenograft assay the present study also demonstrated that CAF-derived exosomes containing miR-29b-1-5p inhibitor dampened tumor growth, VM formation, and EMT-related markers via the VSIG1/ZO-1 axis.

Collectively, we provide evidence that CAFs can secrete miR-29b-1-5p-enriched exosomes into the tumor microenvironment to affect GC progression. Specifically, downregulation of exosomal miR-29b-1-5p in CAFs can target and increase the expression of VSIG1, which then enhances the interaction between VSIG1 and ZO-1, and finally inhibits the VM formation, migration, invasion and EMT process of GC. This study may provide a partial theoretical basis for the clinical development of new targets for GC therapy.

## Disclosure statement

No potential conflict of interest was reported by the author(s).

## Funding

This work was supported by Minhang District Talent Development Special Fund Project (2020) and The Natural Science Foundation of Shanghai Science and Technology Commission [Grant Number: 19ZR1446100].

## Data availability statement

The analyzed data sets generated during the study are available from the corresponding author on reasonable request.

## References

- [1] Johnston FM, Beckman M. Updates on management of gastric cancer. *Curr Oncol Rep.* 2019 Jun 24;21(8):67. PubMed PMID: 31236716. doi: [10.1007/s11912-019-0820-4](https://doi.org/10.1007/s11912-019-0820-4)
- [2] Tan Z. Recent advances in the surgical treatment of advanced gastric cancer: a review. *Med Sci Monit.* 2019 May 13;25:3537–3541. PubMed PMID: 31080234; PubMed Central PMCID: PMC6528544. doi: [10.12659/MSM.916475](https://doi.org/10.12659/MSM.916475)
- [3] Nienhuser H, Schmidt T. Angiogenesis and anti-angiogenic therapy in gastric cancer. *Int J Mol Sci.* 2017 Dec 23;19(1):PubMed PMID: 29295534; PubMed Central PMCID: PMC65795993. doi: [10.3390/ijms19010043](https://doi.org/10.3390/ijms19010043)
- [4] Zhang J, Qiao L, Liang N, et al. Vasculogenic mimicry and tumor metastasis. *J Buon.* 2016 May-Jun;21(3):533–541. PubMed PMID: 27569069.
- [5] Xiang T, Lin YX, Ma W, et al. Vasculogenic mimicry formation in EBV-associated epithelial malignancies. *Nat Commun.* 2018 Nov 27;9(1):5009. PubMed PMID: 30479336; PubMed Central PMCID: PMC6258759. doi: [10.1038/s41467-018-07308-5](https://doi.org/10.1038/s41467-018-07308-5)
- [6] Kim HS, Won YJ, Shim JH, et al. Morphological characteristics of vasculogenic mimicry and its correlation with EphA2 expression in gastric adenocarcinoma. *Sci Rep.* 2019 Mar 4;9(1):3414. PubMed PMID: 30833656; PubMed Central PMCID: PMC6399224. doi: [10.1038/s41598-019-40265-7](https://doi.org/10.1038/s41598-019-40265-7)
- [7] Zeng D, Li M, Zhou R, et al. Tumor microenvironment characterization in gastric cancer identifies prognostic and immunotherapeutically relevant gene signatures. *Cancer Immunol Res.* 2019 May;7(5):737–750. PubMed PMID: 30842092. doi: [10.1158/2326-6066.CIR-18-0436](https://doi.org/10.1158/2326-6066.CIR-18-0436)
- [8] Oya Y, Hayakawa Y, Koike K. Tumor microenvironment in gastric cancers. *Cancer Sci.* 2020 Aug;111(8):2696–2707. PubMed PMID: 32519436; PubMed Central PMCID: PMC7419059. doi: [10.1111/cas.14521](https://doi.org/10.1111/cas.14521)
- [9] Zhai J, Shen J, Xie G, et al. Cancer-associated fibroblasts-derived IL-8 mediates resistance to cisplatin in human gastric cancer. *Cancer Lett.* 2019 Jul 10 PubMed PMID: 30978440;454:37–43. doi: [10.1016/j.canlet.2019.04.002](https://doi.org/10.1016/j.canlet.2019.04.002)
- [10] Ma Z, Chen M, Yang X, et al. The role of cancer-associated fibroblasts in tumorigenesis of gastric cancer. *Curr Pharm Des.* 2018;24(28):3297–3302. PubMed PMID: 29852862. doi: [10.2174/1381612824666180601094056](https://doi.org/10.2174/1381612824666180601094056)
- [11] Miki Y, Yashiro M, Moyano-Galceran L, et al. Crosstalk between cancer associated fibroblasts and cancer cells in scirrhous type gastric cancer. *Front Oncol* [PubMed PMID: 33178597; PubMed Central PMCID: PMC67596590]. 2020;10:568557. doi: [10.3389/fonc.2020.568557](https://doi.org/10.3389/fonc.2020.568557)
- [12] Deng Z, Wu J, Xu S, et al. Exosomes-microRNAs interacted with gastric cancer and its microenvironment: a mini literature review. *Biomarker Med.* 2020 Feb;14(2):141–150. PubMed PMID: 32064893. doi: [10.2217/bmm-2019-0387](https://doi.org/10.2217/bmm-2019-0387)
- [13] Deng G, Qu J, Zhang Y, et al. Gastric cancer-derived exosomes promote peritoneal metastasis by destroying the mesothelial barrier. *FEBS Lett.* 2017 Jul;591(14):2167–2179. PubMed PMID: 28643334. doi: [10.1002/1873-3468.12722](https://doi.org/10.1002/1873-3468.12722)
- [14] Melo SA, Sugimoto H, O'Connell JT, et al. Cancer exosomes perform cell-independent microRNA biogenesis and promote tumorigenesis. *Cancer Cell.* 2014 Nov 10;26(5):707–721. PubMed PMID: 25446899;

- PubMed Central PMCID: PMCPMC4254633. doi: [10.1016/j.ccell.2014.09.005](https://doi.org/10.1016/j.ccell.2014.09.005)
- [15] Liu F, Bu Z, Zhao F, et al. Increased T-helper 17 cell differentiation mediated by exosome-mediated microRNA-451 redistribution in gastric cancer infiltrated T cells. *Cancer Sci.* 2018 Jan;109(1):65–73. PubMed PMID: 29059496; PubMed Central PMCID: PMCPMC5765284. doi: [10.1111/cas.13429](https://doi.org/10.1111/cas.13429)
- [16] Yang H, Fu H, Wang B, et al. Exosomal miR-423-5p targets SUFU to promote cancer growth and metastasis and serves as a novel marker for gastric cancer. *Mol Carcinog.* 2018 Sep;57(9):1223–1236. PubMed PMID: 29749061. doi: [10.1002/mc.22838](https://doi.org/10.1002/mc.22838)
- [17] Kim S, Bae WJ, Ahn JM, et al. MicroRNA signatures associated with lymph node metastasis in intramucosal gastric cancer. *Mod Pathol.* 2021 Mar;34(3):672–683. PubMed PMID: 32973329. doi: [10.1038/s41379-020-00681-x](https://doi.org/10.1038/s41379-020-00681-x)
- [18] Kurihara-Shimomura M, Sasahira T, Shimomura H, et al. The oncogenic activity of miR-29b-1-5p induces the epithelial-mesenchymal transition in oral squamous cell carcinoma. *J Clin Med.* 2019 Feb 24;8(2). doi: [10.3390/jcm8020273](https://doi.org/10.3390/jcm8020273). PubMed PMID: 30813466; PubMed Central PMCID: PMCPMC6406827.
- [19] Chen Y, Pan K, Li S, et al. Decreased expression of V-set and immunoglobulin domain containing 1 (VSIG1) is associated with poor prognosis in primary gastric cancer. *J Surg Oncol.* 2012 Sep 1;106(3):286–293. PubMed PMID: 22095633. doi: [10.1002/jso.22150](https://doi.org/10.1002/jso.22150)
- [20] Zhang H, Deng T, Liu R, et al. CAF secreted miR-522 suppresses ferroptosis and promotes acquired chemo-resistance in gastric cancer. *Mol Cancer.* 2020 Feb 27;19(1):43. PubMed PMID: 32106859; PubMed Central PMCID: PMCPMC7045485. doi: [10.1186/s12943-020-01168-8](https://doi.org/10.1186/s12943-020-01168-8)
- [21] Kang L, Shen L, Lu L, et al. Asparaginyl endopeptidase induces endothelial permeability and tumor metastasis via downregulating zonula occludens protein ZO-1. *Biochim Biophys Acta Mol Basis Dis.* 2019 Sep 1;1865(9):2267–2275. PubMed PMID: 31096007. doi: [10.1016/j.bbadis.2019.05.003](https://doi.org/10.1016/j.bbadis.2019.05.003)
- [22] Kim E, Lee Y, Kim JS, et al. Extracellular domain of V-set and immunoglobulin domain containing 1 (VSIG1) interacts with sertoli cell membrane protein, while its PDZ-binding motif forms a complex with ZO-1. *Mol Cells.* 2010 Nov;30(5):443–448. PubMed PMID: 20957455. doi: [10.1007/s10059-010-0138-4](https://doi.org/10.1007/s10059-010-0138-4)
- [23] Yang F, Ning Z, Ma L, et al. Exosomal miRNAs and miRNA dysregulation in cancer-associated fibroblasts. *Mol Cancer.* 2017 Aug 29;16(1):148. PubMed PMID: 28851377; PubMed Central PMCID: PMCPMC5576273. doi: [10.1186/s12943-017-0718-4](https://doi.org/10.1186/s12943-017-0718-4)
- [24] Schoepp M, Stroese AJ, Haier J. Dysregulation of miRNA expression in cancer associated fibroblasts (CAFs) and its consequences on the tumor microenvironment. *Cancers (Basel).* 2017 May 24;9(12):54. PubMed PMID: 28538690; PubMed Central PMCID: PMCPMC5483873. doi: [10.3390/cancers9060054](https://doi.org/10.3390/cancers9060054)
- [25] Kim YJ, Hwang KC, Kim SW, et al. Potential miRNA-target interactions for the screening of gastric carcinoma development in gastric adenoma/dysplasia. *Int J Med Sci.* 2018;15(6):610–616. PubMed PMID: 29725252; PubMed Central PMCID: PMCPMC5930463. doi: [10.7150/ijms.24061](https://doi.org/10.7150/ijms.24061)
- [26] Kim YJ, Jeong S, Jung WY, et al. miRNAs as potential biomarkers for the progression of gastric cancer inhibit CREBZF and regulate migration of gastric adenocarcinoma cells. *Int J Med Sci.* 2020;17(6):693–701. PubMed PMID: 32218690; PubMed Central PMCID: PMCPMC7085260. doi: [10.7150/ijms.42654](https://doi.org/10.7150/ijms.42654)
- [27] Inoue A, Mizushima T, Wu X, et al. A miR-29b byproduct sequence exhibits potent tumor-suppressive activities via inhibition of NF-kappaB signaling in KRAS-Mutant colon cancer cells. *Mol Cancer Ther.* 2018 May;17(5):977–987. PubMed PMID: 29545333. doi: [10.1158/1535-7163.MCT-17-0850](https://doi.org/10.1158/1535-7163.MCT-17-0850)
- [28] De Blasio A, Di Fiore R, Pratelli G, et al. A loop involving NRF2, miR-29b-1-5p and AKT, regulates cell fate of MDA-MB-231 triple-negative breast cancer cells. *J Cell Physiol.* 2020 Feb;235(2):629–637. PubMed PMID: 31313842. doi: [10.1002/jcp.29062](https://doi.org/10.1002/jcp.29062)
- [29] Wang H, Wei H, Wang J, et al. MicroRNA-181d-5p-containing exosomes derived from CAFs promote EMT by regulating CDX2/HOXA5 in breast cancer. *Mol Ther Nucleic Acids.* 2020 Mar 6;19:654–667. PubMed PMID: 31955007; PubMed Central PMCID: PMCPMC6970169. doi: [10.1016/j.omtn.2019.11.024](https://doi.org/10.1016/j.omtn.2019.11.024)
- [30] Hu JL, Wang W, Lan XL, et al. CAFs secreted exosomes promote metastasis and chemotherapy resistance by enhancing cell stemness and epithelial-mesenchymal transition in colorectal cancer. *Mol Cancer.* 2019 May 7;18(1):91. PubMed PMID: 31064356; PubMed Central PMCID: PMCPMC6503554. doi: [10.1186/s12943-019-1019-x](https://doi.org/10.1186/s12943-019-1019-x)
- [31] Inoue Y, Matsuura S, Yoshimura K, et al. Characterization of V-set and immunoglobulin domain containing 1 exerting a tumor suppressor function in gastric, lung, and esophageal cancer cells. *Cancer Sci.* 2017 Aug;108(8):1701–1714. PubMed PMID: 28603843; PubMed Central PMCID: PMCPMC5543479. doi: [10.1111/cas.13295](https://doi.org/10.1111/cas.13295)
- [32] Gurzu S, Sugimura H, Szederjesi J, et al. Interaction between cadherins, vimentin, and V-set and immunoglobulin domain containing 1 in gastric-type hepatocellular carcinoma. *Histochem Cell Biol.* 2021 Oct;156(4):377–390. PubMed PMID: 34170400. doi: [10.1007/s00418-021-02006-8](https://doi.org/10.1007/s00418-021-02006-8)
- [33] Yokota Y, Noda T, Okumura Y, et al. Serum exosomal miR-638 is a prognostic marker of HCC via downregulation of VE-cadherin and ZO-1 of endothelial cells. *Cancer Sci.* 2021 Mar;112(3):1275–1288.

- PubMed PMID: 33426736; PubMed Central PMCID: PMC7935782. doi: [10.1111/cas.14807](https://doi.org/10.1111/cas.14807)
- [34] Zhang X, Wang L, Zhang H, et al. Decreased expression of ZO-1 is associated with tumor metastases in liver cancer. *Oncol Lett.* 2019 Feb;17(2):1859–1864. PubMed PMID: 30675248; PubMed Central PMCID: PMC6341828. doi: [10.3892/ol.2018.9765](https://doi.org/10.3892/ol.2018.9765)
- [35] Liu M, Yang J, Zhang Y, et al. ZIP4 promotes pancreatic cancer progression by repressing ZO-1 and Claudin-1 through a ZEB1-dependent transcriptional mechanism. *Clin Cancer Res.* 2018 Jul 1;24(13):3186–3196. PubMed PMID: 29615456; PubMed Central PMCID: PMC67006048. doi: [10.1158/1078-0432.CCR-18-0263](https://doi.org/10.1158/1078-0432.CCR-18-0263)
- [36] Chen X, Zhao M, Huang J, et al. MicroRNA-130a suppresses breast cancer cell migration and invasion by targeting FOSL1 and upregulating ZO-1. *J Cell Biochem.* 2018 Jun;119(6):4945–4956. PubMed PMID: 29384218. doi: [10.1002/jcb.26739](https://doi.org/10.1002/jcb.26739)
- [37] Hsu YL, Hung JY, Chang WA, et al. Hypoxic lung cancer-secreted exosomal miR-23a increased angiogenesis and vascular permeability by targeting prolyl hydroxylase and tight junction protein ZO-1. *Oncogene.* 2017 Aug 24;36(34):4929–4942. PubMed PMID: 28436951. doi: [10.1038/onc.2017.105](https://doi.org/10.1038/onc.2017.105)